

Optical limiting in a periodic materials with relaxational nonlinearity

Xue Liu,^{1,2} Joseph W. Haus^{1,*} and M. S. Shahriar²,

¹*Electro-Optics Program, University of Dayton, 300 College Park, Dayton, OH 45469-0245, USA*

²*Electrical Engineering and Computer Science, Northwestern University, 2145 N. Sheridan Road, Evanston, IL 60208, USA*

*Corresponding author: Joseph.Haus@notes.udayton.edu

Abstract: We numerically investigate counter-propagating beams in a one-dimensionally, periodic structure with non-instantaneous Kerr nonlinearity for the design of efficient optical limiters. The performance of the Photonic Band Gap optical limiter with different response times is compared with the instantaneous case. Dynamic range and the cutoff intensity can be improved over a range of relaxation times.

© 2009 Optical Society of America

OCIS codes: 190.3100 Instabilities and chaos; 190.4420 Nonlinear optics, transverse effects in; 190.5940 Self-action effects.

References and links

1. T. Xia, D. J. Hagan, A. Dogariu, A. A. Said, and E. W. Van Stryland, "Optimization of optical limiting devices based on excited-state absorption," *Appl. Opt.* **36**, 4110-4122 (1997).
2. J. S. Shirk, R. G. S. Pong, F. J. Bartoli, and A. W. Snow, "Optical limiter using a lead phthalocyanine," *Appl. Phys. Lett.* **63**, 1880-1882 (1993).
3. J. Shirk, R. Pong, S. Flom, F. Bartoli, M. Boyle, and A. Snow, "Lead phthalocyanine reverse saturable absorption optical limiters," *Pure Appl. Opt.* **5**, 701-707 (1996).
4. P. Tran, "All-optical switching with a nonlinear chiral photonic bandgap structure," *J. Opt. Soc. Am. B* **16**, 70-73 (1999).
5. J. P. Dowling, M. Scalora, M. J. Bloemer and C. M. Bowden, "The photonic band edge laser: A new approach to gain enhancement," *J. Appl. Phys.* **75**, 1896-1899 (1994).
6. M. Scalora, J. P. Dowling, M. J. Bloemer and C. M. Bowden, "The photonic band edge optical diode," *J. Appl. Phys.* **76**, 2023-2026 (1994).
7. M. Scalora, J.P. Dowling, C.M. Bowden and M. J. Bloemer, "Optical limiting and switching of ultrashort pulses in nonlinear photonic band gap materials," *Phys. Rev. Lett.* **73**, 1368-1371 (1994).
8. M. Scalora, N. Mattiucci, G. D'Aguanno, M. C. Larciprete, and M. J. Bloemer, "Nonlinear pulse propagation in one-dimensional metal-dielectric multilayer stacks: Ultrawide bandwidth optical limiting," *Phys. Rev. E* **73**, 016603 (2006).
9. B. Y. Soon and J. W. Haus, "One-dimensional photonic crystal optical limiter," *Opt. Express* **11**, 2007-2018 (2003).
10. B. J. Eggleton, C. M. deSterke, R. E. Slusher and J. E. Sipe, "Distributed feedback pulse generator based on nonlinear fiber grating," *Electron. Lett.* **32**, 2341-2342 (1996).
11. J. W. Haus, B. Y. Soon, M. Scalora, C. Sibilila, I. Mel'nikov, "Coupled-mode equations for Kerr media with periodically modulated linear and nonlinear coefficients," *J. Opt. Soc. Am. B* **19**, 2282-2291 (2002).
12. J. W. Haus, B. Y. Soon, M. Scalora, M. Bloemer, C. Bowden, C. Sibilila, and A. Zheltikov, "Spatiotemporal instabilities for counter-propagating waves in periodic media," *Opt. Express* **10**, 114-121 (2002).
13. M. Mitchell, Z. Chen, M. F. Shih, and M. Segev, "Self-trapping of partially spatially incoherent light," *Phys. Rev. Lett.* **77**, 490-493 (1996).
14. X. Liu, J. W. Haus and S.M. Shahriar, "Modulation instability for a relaxational Kerr medium," *Opt. Commun.* **281**, 2907-2912 (2008).
15. M.-F. Shih, C.-C. Jeng, F.-W. Sheu, and C.-Y. Lin, "Spatiotemporal Optical Modulation Instability of Coherent Light in Noninstantaneous Nonlinear Media," *Phys. Rev. Lett.* **88**, 133902 (2002).

1. Introduction

One of the key challenges in the development of optical limiters is the search for appropriate materials that rapidly respond to the applied laser intensity, have good nonlinear absorption characteristics over a broad range of wavelengths and have a high damage threshold. To protect the eyes the transmitted fluence through the device should be clamped under 500 nJ/cm^2 over a range of visible wavelengths. Dangerous IR radiation could be eliminated by a fixed high pass filter. Organic materials have shown great promise for optical limiting applications. They possess reverse saturable absorber action where molecules are designed to possess larger excited-state absorption than ground-state absorption. The principal feature is their enhanced nonlinear absorption at higher intensities, but they also have nonlinear refraction effects [1]. The spectral range of materials can be engineered to cover bands. Lead phthalocyanines have absorption bands that can cover the visible and near-IR regimes [2,3].

One dimensional Photonic Band Gap (PBG) structures have been proposed as a fabrication strategy to improve the optical limiting performance of materials. The unusual spatial and temporal dispersion properties of PBGs make them excellent candidates for manipulating the dispersion characteristics of the composite material. This has given rise to a wide range of proposed photonic devices [4-8], among which nonlinear PBG optical limiters have emerged as showing potential due to their compact structure and straightforward fabrication process.

Earlier work on PBG optical limiters was based on exploiting transverse and longitudinal modulation instabilities using Kerr media [9]. Compared with traditional homogeneous nonlinear optical limiters, this design has shown promising performance for optical limiting, i.e., high transmission for normal light and low for intense beams, effective in protecting optical elements and sensors against damage by exposure to malicious or unexpected high-intensity light.

The PBG can provide access to the nonlinearity of materials, such as metals, that are not normally considered as candidates for optical limiting materials. Scalora et al. recently developed a chirped PBG device with copper layers to induce broadband optical limiting [8]. The chirped dielectric layer thicknesses are designed to improve the linear transmittance and concentrate large fields inside the copper to access the large nonlinearity. An added advantage is that the stack filters the rest of the spectrum outside the visible regime.

In this paper, the counter-propagating waves in one dimensional PBG structure with relaxational nonlinearity are numerically investigated. The role of the spatial and temporal modulation instabilities on reshaping the forward and backward fields as a function of the relaxation time is elucidated. The finite response time of the Kerr effect is taken into consideration in the model. Based on the nonlinear, defocusing effect of the modulation instabilities, an optical limiter is exploited by placing an aperture in the far field behind the PBG structure. The role of nonlinear response time on the performance of optical limiter is examined.

2. Mode-coupled equations and computational approach

The dynamical equations for counter-propagating waves in a non-instantaneous nonlinear PBG structure can be derived by applying the multiple scales method to the classical nonlinear wave equation [10]. The dynamics of the medium is described by a simple relaxational model with the medium's response time.

$$\frac{1}{v} \frac{\partial E_f}{\partial t} = -\frac{\partial E_f}{\partial z} + \frac{i}{F} \Delta_{\perp}^2 E_f + i\delta E_f + i\kappa E_b + i\eta N_f E_f, \quad (1-a)$$

$$\frac{1}{v} \frac{\partial E_b}{\partial t} = \frac{\partial E_b}{\partial z} + \frac{i}{F} \Delta_{\perp}^2 E_b + i\delta E_b + i\kappa E_f + i\eta N_b E_b, \quad (1-b)$$

$$\frac{\partial N_f}{\partial t} = \frac{1}{\tau} (-N_f + |E_f|^2 + 2|E_b|^2), \quad (1-c)$$

$$\frac{\partial N_b}{\partial t} = \frac{1}{\tau} (-N_b + |E_b|^2 + 2|E_f|^2), \quad (1-d)$$

where the fields $E_f = E_f(x, z, t)$ and $E_b = E_b(x, z, t)$ describe the electric field envelope of the forward and backward waves in space and time. We denote by x the transverse coordinate, since we will treat only a single transverse dimension in our PBG structure; v denotes group velocity, F is the Fresnel parameter, $\delta = k - k_0$ stands for the detuning of the initial pulse wave number from the center of the stop band, and $k_0 = \frac{\pi}{\Lambda}$ where Λ is the lattice constant. κ denotes the coupling coefficient of the grating, and η is the nonlinear Kerr coefficient, which is assumed homogeneous throughout the medium. In our numerical model, the index change of the two materials is assumed to be weakly periodic. N_f and N_b represent the excitation densities of the nonlinear medium for the forward and backward waves, respectively. The finite response time of the Kerr effect of the PBG structure is denoted by τ . From Eqs. (1c) and (1d) it is clear that the dynamics of N is not only related to the local field intensities of both waves, but also the response time of the medium.

We consider the case that the signal is only launched into one side of the PBG structure. Therefore, the boundary conditions we applied to the model are

$$E_f(x, 0, t) = E_f(x, t) \quad (2-a)$$

$$E_b(x, L, t) = 0 \quad (2-b)$$

In our previous research [11], a novel split-step method has been introduced to solve Eq. (1). By separating the propagation into 2x2 matrices, we express Eq. (1) in the symbolic matrix form

$$\frac{dU}{dt} = (\tilde{L} + \tilde{N})U, \quad (3)$$

where the state vector is

$$U = (E_f, E_b)^T, \quad (4)$$

and the operators are

$$\tilde{L} = \begin{pmatrix} -\frac{\partial}{\partial z} + \frac{i}{F} \Delta_{\perp}^2 + i\delta & 0 \\ 0 & -\frac{\partial}{\partial z} + \frac{i}{F} \Delta_{\perp}^2 + i\delta \end{pmatrix} + \begin{pmatrix} 0 & i\kappa \\ i\kappa & 0 \end{pmatrix} = \tilde{V} + \tilde{K}, \quad (5-a)$$

$$\tilde{N} = \begin{pmatrix} i\eta N_f & 0 \\ 0 & i\eta N_b \end{pmatrix}. \quad (5-b)$$

Matrices L and N , representing the linear and nonlinear parts of the partial-differential

equation, are treated differently in separate steps.

For the linear step, because the operator L can be decomposed into a diagonal and an off-diagonal matrix, we can further simplify the calculations if the step size is small enough. i.e.

$$U_L(t + \frac{dt}{2}) = \exp(\frac{Vdt}{2}) \exp(\frac{Kdt}{2}) U(t) \quad (6)$$

where the subscript L stands for the linear propagation contribution. Equation (6) can be readily solved in the Fourier space. In our calculation, 2048 and 1024 points are used for Fast Fourier Transform in the longitudinal and transverse directions, respectively. For the nonlinear step, we first find the analytical solutions for Eqs. (1c) and (1d)

$$N_f(x, z, t) = \frac{1}{\tau} \int_{-\infty}^t e^{-\frac{(t-t')}{\tau}} (2|E_b(x, z, t')|^2 + |E_f(x, z, t')|^2) dt' \quad (7-a)$$

$$N_b(x, z, t) = \frac{1}{\tau} \int_{-\infty}^t e^{-\frac{(t-t')}{\tau}} (2|E_f(x, z, t')|^2 + |E_b(x, z, t')|^2) dt' \quad (7-b)$$

By assuming that N_f and N_b stay constant for a small step size, the solution to the nonlinear step can be written as

$$U_N(t + \frac{dt}{2}) = \exp(Ndt) U(t) \quad (8)$$

where the subscript N refers to the nonlinear contribution to the propagation.

Combining the two separated steps together, the second-order solution for U at the incremented time $t + dt$ is

$$U(t + dt) = \exp(\frac{Vdt}{2}) \exp(\frac{Kdt}{2}) \exp(Ndt) \exp(\frac{Vdt}{2}) \exp(\frac{Kdt}{2}) U(t) \quad (9)$$

We monitor the accuracy of the numerical method by examining the law of energy conversation at each time step.

3. Results

3.1. Propagation

The forward propagating pulse is placed outside the PBG structure at certain distance z_0 so that the initial field in the PBG structure vanishes. The intensity distribution of the pulse is in a Gaussian shape transversely and longitudinally, i.e.

$$E_f(x, z, 0) = A \exp(-(z - z_0)^2 / \sigma_z^2) \exp(-x^2 / \sigma_x^2) \quad (10)$$

The initial condition for the backward propagating pulse is

$$E_b(x, z, 0) = 0 \quad (11)$$

To simplify the calculations, the parameters in Eq. (1) are scaled as follows: $v = 1, \kappa = 1, \eta = 1$. We tune the incident laser pulse central angular frequency away from the center of the PBG stop band by changing the value of δ . The selection of δ is closely related to the spatio-temporal modulation instability of the nonlinear PBG structure, which is essential in influencing the propagation of the pulse. When the first transmission peak of the PBG for positive angular frequency, also called the “band-edge”, overlaps with the center of the pulse spectrum the break-up of the pulse is maximized by the spatio-temporal modulation instability

[12]. The transmission curve for the PBG structure used in our simulation with a length $L=6.1$ is plotted in Fig. 1. The offset from the center of the pulse spectrum to the band-edge of the PBG is $\delta = 1.12$,

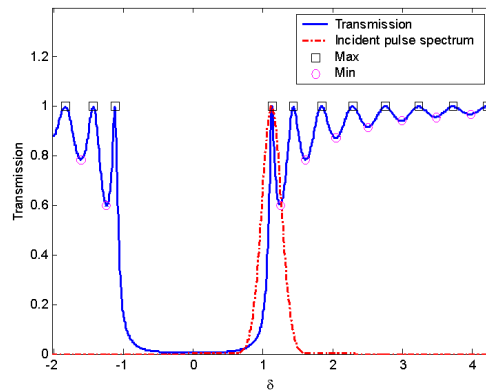


Fig. 1. Transmission curve of the PBG structure and the spectrum of the input pulse.

Previous papers show that the threshold of initial amplitude for modulation instability to occur is around $A=0.3$. In our simulations, we set the amplitude at $A=0.75$, to ensure a high modulation instability gain. The different nonlinear response time chosen for the PBG structure are $\tau_1 = 0.1$, $\tau_2 = 1$ and $\tau_3 = 4$. The case for an instantaneous PBG structure is also simulated for comparison.

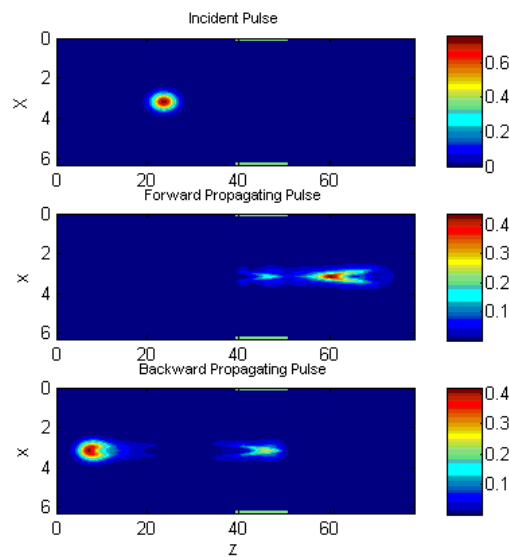


Fig. 2(a). A snapshot of the pulse evolution through an instantaneous nonlinear medium placed in a PBG. Top frame is the initial pulse, which is launched outside the medium. The central frame and bottom frame are the forward propagating and backward propagating pulse, respectively. The initial amplitude of the wave is $A=0.75$.

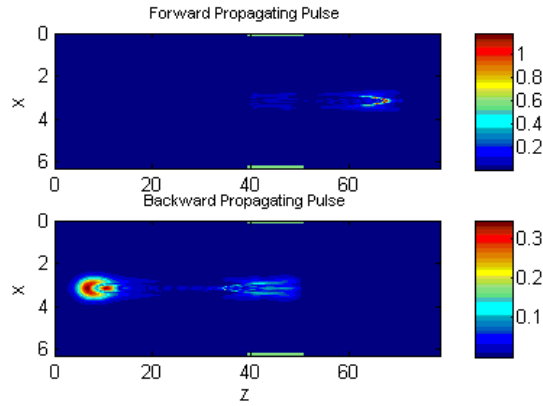


Fig. 2(b). A snapshot of the forward- and backward waves with a non-instantaneous nonlinear medium embedded in the PBG. The relaxation time is $\tau_1 = 0.1$ and the amplitude is the same as in Fig. 2(a).

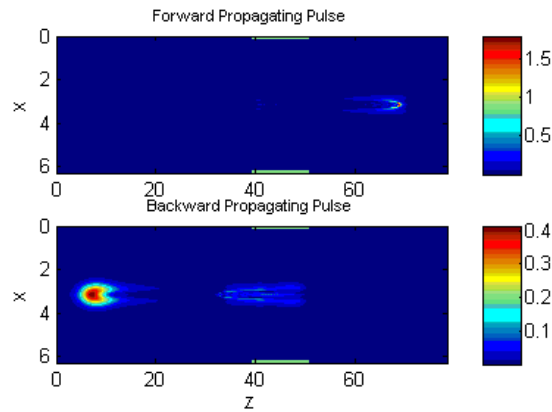


Fig. 2(c). A snapshot of the forward- and backward waves with a non-instantaneous nonlinear medium embedded in the PBG. The relaxation time is $\tau_2 = 1$ and the amplitude is the same as in Fig. 2(a).

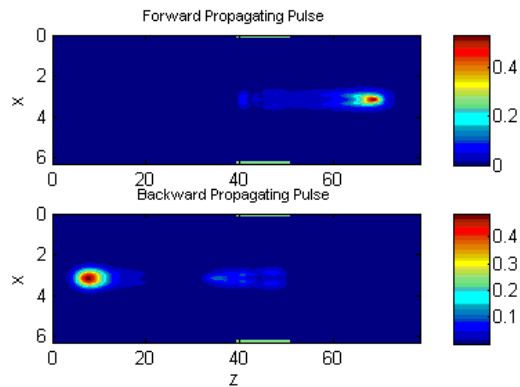


Fig. 2(d). A snapshot of the forward- and backward waves with a non-instantaneous nonlinear medium embedded in the PBG. The relaxation time is $\tau_3 = 4$ and the amplitude is the same as in Fig. 2(a).

Snapshot views of the pulse forward-backward pulse intensities for different relaxation times are shown in Figs. 2(a)-2(d). The position of the PBG medium is denoted by a pair of green bars placed between the range $z=(40,50)$. The absolute amplitude of the field at each pixel is represented by a color with the amplitude shown in the vertical scale on the right side. The vertical axis displays the transverse coordinate and the horizontal axis is the propagation direction.

The top figure is the input Gaussian field; its pulse width is shorter than the medium so that it samples a large portion of the dispersive spectrum in the medium. The middle figure is the continuation of the forward-propagating pulse as it passes into and through the PBG sample. The bottom figure shows the propagation of the backward propagating pulse in the medium. In our computations F is chosen to be extremely large ($F=10^7$) so that the transverse coupling is weak and does not noticeably affect the pulse tuning at a selected frequency. Comparison among Figs. 2(a) through 2(d) leads to several observations about the effect of the non-instantaneous nonlinear PBG structure on pulse propagation. In all four cases, the forward propagating pulse with initial Gaussian profile undergoes a strong distortion inside the medium. For the instantaneous case, the modulation instability leads to a rapid anomalous spread of the pulse in both transverse and longitudinal directions, which demonstrates that phase changes of the beam in the transverse direction are sufficient to modulate the amplitude by the end of the medium. For a short response time ($\tau=0.1$), not only does the profile of the forward propagating pulse undergo a major distortion into an arch-like shape, but also the energy redistribution in both transverse and longitudinal directions becomes discontinuous. The intensity peaks appear at discrete spots, which can be readily seen in the 3-D plot of Fig. 3. A close look at the forward propagating pulse shows that more high frequency components exist than in the case of an instantaneous nonlinear PBG structure. This phenomenon can be explained by interpreting the Modulation Instability as a degenerated form of Four Wave Mixing in the Kerr medium, the perturbation being the probe and the CW pump beam [13]. The energy of the two photons from the pump produces two new conjugate frequency photons. In the instantaneous case, to generate MI, phase-match condition is required from the pump and the probe, thus the generated frequency is strictly limited. But when the medium response time is taken into account, a Raman-like nonlinearity is developed for which self-phase-match is achieved, leading to a gain region outside the original sideband.

Previous studies show that the finite response time of the Kerr effect alters the MI by lowering the gain and removing the gain cutoff frequency [14,15]. For a short response time, the overall gain for small perturbations is only slightly decreased, but the whole gain region is widely extended, leading to a stronger break-up of the pulse. In the sub frame for the backward propagating wave, we also observe an arch-like but weaker distortion than the forward propagating wave due to the limited passage in the nonlinear PBG structure. A rib structure is displayed which is also a characteristic of the longitudinal modulation instability.

As seen from Fig. 2(c), even for $\tau=1$, the reshaping of both the forward and backward propagating waves into an arch pattern can still be observed. The distortion and rib structures are less obvious due to the weaker modulation instability.

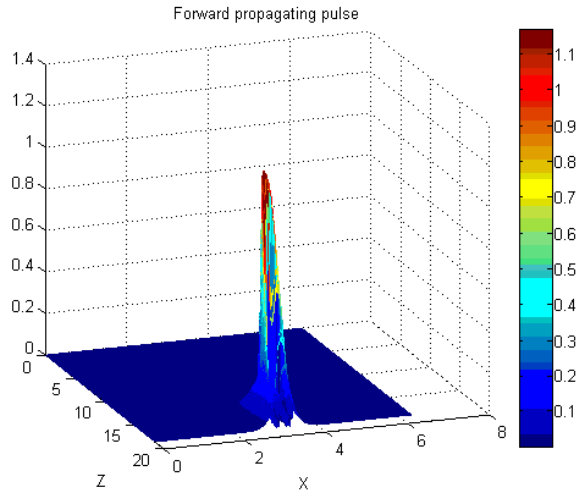


Fig. 3. 3-D plot of the forward propagating pulse.

As the response time largely increases as in Fig. 2(d) ($\tau = 4$), the pulse shape is only moderately distorted. The reason is that the overall gain that resulted from the modulation instability is greatly lowered by the long response time. The effect of the nonlinearity is abated. Also for the backward propagating pulse, the rib structure of the backward wave almost disappears, which is also a sign of the weak modulation instability.

3.2 Optical limiting

The ability of the non-instantaneous nonlinear PBG structure to break up a pulse makes itself a promising candidate for optical limiting. Since the energy of the incident pulse is spread longitudinally and transversely by the modulation instability, we place an aperture in the Fraunhofer regime after the PBG structure to further enhance the optical limiting as shown in Fig. 4. The size of the aperture is set to be the FWHM of the initial pulse, such that when the intensity is low, most part of the optical pulse is passed, and when the intensity gets undesirably high, a large portion of the spread optical beam is clipped. A probe is positioned behind the aperture to detect the transmitted energy.

Aperture placed behind the PBG structure in the far field

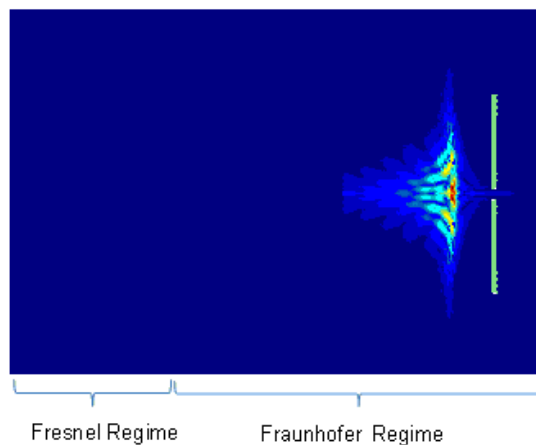


Fig. 4. Aperture placed in the Fraunhofer regime to block out energy flow ($A = 0.75, \tau = 1$). The Fresnel number is $F = 10^7$.

In order to evaluate the performance of the optical limiter, certain criteria need to be set up for comparison. Two figures of merit are proposed to categorize the performance of optical limiters. First, we define the transmission dynamic range (TDR) to be

$$\text{TDR} = \psi = \frac{T_{\max}}{T_{\min}} \quad (12)$$

Note that if T_{\min} is zero, TDR is infinite for any nonzero T_{\max} . Generally, TDR is more sensitive to the change in T_{\max} . We define a second figure of merit related to the transmission cutoff (TCO) response band; it is defined by the intensity difference between the normalized 20% and 80% transmission points, i.e.

$$\text{TCO} = \frac{T_{80\%} - T_{20\%}}{T_{80\%} + T_{20\%}} \quad (13)$$

TCO shows how fast the transmission drops at the cut-off point. The smaller TCO is, the closer it approaches the ideal optical limiter.

Generally, an ideal optical limiter performance is approached as $\text{TDR} \rightarrow \infty$ and $\text{TCO} = 0$.

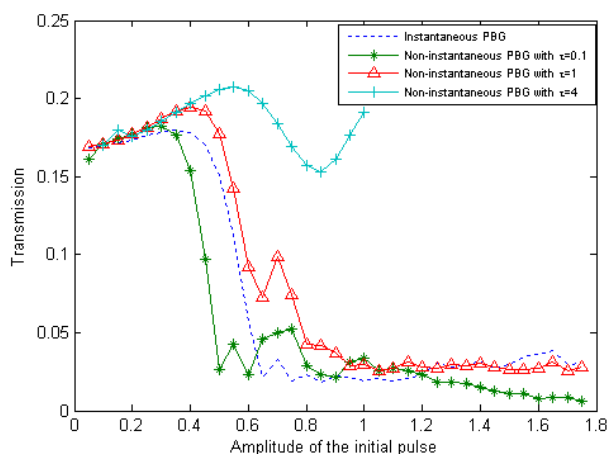


Fig. 5. Transmission curves for PBG structures with different response time.

Table 1, The figures of merit for instantaneous and non-instantaneous nonlinear media embedded in a PBG optical limiter.

Relaxation time	TDR	TCO
$\tau = 0$ (Instantaneous)	9.8004	0.209
$\tau = 0.1$	28.9355	0.190
$\tau = 1$	7.6128	0.465
$\tau = 4$	1.3556	N/A

Figure 5 summarizes the transmission characteristics for the non-instantaneous medium distributed in a PBG. We note that for a small response time ($\tau = 0.1$) the wave has a higher T_{\max} , lower T_{\min} and decays faster than the instantaneous PBG. In terms of figures of merit, the optical limiting performance is improved in all aspects: higher TDR and lower TCO as shown in Table 1. Even for relatively long response time $\tau = 1$, the optical limiting properties are comparable to the instantaneous case. But for a PBG structure with a long response time ($\tau = 4$), due to the weak modulation instability gain, the break-up of the pulse in the far field is dramatically suppressed, which reduces the optical limiting performance.

4. Conclusion

In this paper, we presented a numerical model for counter-propagating waves in the one dimensional non-instantaneous nonlinear PBG structure. The case that the pulse is incident from one side of the PBG structure is especially stressed. The band-edge of the photonic crystal is manipulated to overlap with the center of the spectrum of the incident pulse to maximize the modulation instability. Our study shows that a small finite response time of the Kerr effect ($\tau = 0.1$) of the PBG can strengthen the spatio-temporal modulation instability of the medium, leading to a rapid spread of the pulse in the transverse direction and stronger temporal break-up of the pulse above threshold intensity. For relaxation times of the order unity the performance of our optical limiter is not degraded over the instantaneous case. High frequency components are observed due to the extended “gain region” of the modulation instability, which leads to additional performance improvements for optical limiting applications. However, for long relaxation times, the nonlinear effect is weakened by lower

gain of the modulation instability.

In Section 3 we applied the spatio-temporal modulation instability in non-instantaneous nonlinear PBG to design an optical limiter. An aperture is placed in far-field to filter high-intensity light before entering the detector. The performance of our design is evaluated in terms of the dynamic range (TDO) and the transmission cutoff (TCO). It is found that both figures of merit are improved in the case where the response time is short ($\tau = 0.1$) compared to the pulse duration, which shows promising optical limiting characteristics. It is also found that material with long Kerr relaxational response times is not suitable for our design.

The optical limiter can be further improved by optimizing the parameters in the system. The other factors that we can modify to further improve the performance of the optical limiter include the aperture size, the length of the PBG structure, the complex third-order nonlinearity of the medium and the diffraction parameter F , beam focusing in the medium, and the beam shape. Based on earlier publications, longer pulses should experience better optical limiting.